Assembly of Printed Interconnects for Immobilized Protein Microfluidic Assays

Qianwen Xu
Smart Manufacturing Thrust
Systems Hub
Hong Kong University of Science and Technology
Hong Kong, China
qxuak@connect.ust.hk

S. W. Ricky Lee*
Smart Manufacturing Thrust
Systems Hub
Hong Kong University of Science and Technology
Guangzhou, China
HKUST Shenzhen-Hong Kong Collaborative Innovation Research Institute
*rickylee@ust.hk

Yusong Guo
Division of Life Science
Hong Kong University of Science and Technology
Hong Kong, China
guoyusong@ust.hk

Jeffery C. C. Lo
HKUST Foshan Research Institute for Smart Manufacturing
Hong Kong University of Science and Technology
Hong Kong, China
jefflo@ust.hk

***Abstract*—Microfluidics has attracted significant attention for biological applications, particularly for high-throughput screening and multiplexing. However, conventional interconnect techniques are limited in their ability to fabricate the hundreds or thousands of microfluidic interconnects needed to process multiple samples for high-throughput microfluidics. To address this challenge, coaxial printing was invented to enable rapid, customizable, and scalable microfluidic interconnects. This paper focuses on the assembly process of coaxial printed interconnects for immobilized protein microfluidic assays. We demonstrate the immobilization of protein into a 1 x 1 microwell microfluidic unit with printed connectors to showcase the process.**

Keywords—Microfluidic, Interconnects, High-throughput, 3D Printing, Protein Immobilization

I. INTRODUCTION

The field of microfluidics has experienced rapid growth and has exciting applications in various areas of research and industry, including drug delivery [1], point-of-care diagnostics [2], lab-on-a-chip systems [3], and environmental monitoring [4]. Compared to traditional laboratory methods, microfluidics can reduce sample costs, enhance mass transfer and chemical/biological reactions, and provide highly controlled and precise fluid handling, which can improve the accuracy and reproducibility of analyses [5]. Additionally, microfluidics enables high-throughput screening [6] and multiplexing (see Fig. 1), allowing for the handling of large numbers of samples or compounds. This capability can accelerate the discovery of new drugs or biomarkers and reduce the time and resources required for experiments.

Microfluidics has the potential to revolutionize the way we study and understand biological systems. By enabling the isolation and analysis of individual cells, it provides insights into cellular heterogeneity and function, which is particularly important for applications such as cancer research and regenerative medicine [7]. Moreover, microfluidics is a valuable tool for studying the complex networks of protein interactions that underlie biological processes and for identifying new targets for drug discovery and development. Overall, microfluidics has the potential to greatly enhance our understanding of biological systems and accelerate the discovery of new treatments for diseases.

The fabrication of microfluidic devices relies on microfabrication techniques such as photolithography, replica molding, bonding, and functionalization [8]. These techniques are used to construct channels, chambers, and other features that manipulate fluids at the micro-scale. Surface coatings or other modifications are often necessary to enable specific biological or chemical interactions. For biosensors, biomolecules such as proteins or nucleic acids must be immobilized on the surface using methods such as covalent bonding, physical adsorption, affinity, or entrapment. Covalent bonding is the most efficient immobilization method with various chemistries. Microcontact printing (μCP) [9] is an effective approach to creating desired patterns by transferring the patterns of polydimethylsiloxane (PDMS) stamps to substrates with high resolution and precision.

Reliable interconnects play a vital role in communicating between microfluidic parts, including sample feeding, channel processing, and analysis. In the early days of microfluidics, tubes were manually inserted into chip holes using adhesives [10]. However, due to the lack of precise control, adhesives could spread to channels and cause clogging. Subsequently, adapters such as Luer-lock fittings [11] and clamp fixtures [12] [13] were employed to facilitate interconnection. However, these approaches often have cumbersome interfaces or large pitch sizes, which work for only several or tens of microfluidic connections but face challenges for high-throughput microfluidics with hundreds or thousands of connections. Scalability of microfluidic interconnects is an urgent need when processing multiple samples for high-throughput screening. This means that interconnects must be easily replicated or modified to accommodate different sample volumes or assay formats.

3D printing has the potential to enable rapid and customizable fabrication of microfluidic devices, including interconnects. In our previous works [14] [15], we introduced coaxial printing to print hollow connectors on device orifices, serving as microfluidic interconnects. This approach is fixture-free, scalable, robust, and reliable. In this paper, we focus on the assembly process of printed interconnects for immobilized protein microfluidic assays, as shown in Fig. 2. We immobilize proteins in a 1 x 1 microwell region via covalent bonds and employ microcontact printing to create a single-circle protein pattern for demonstration.

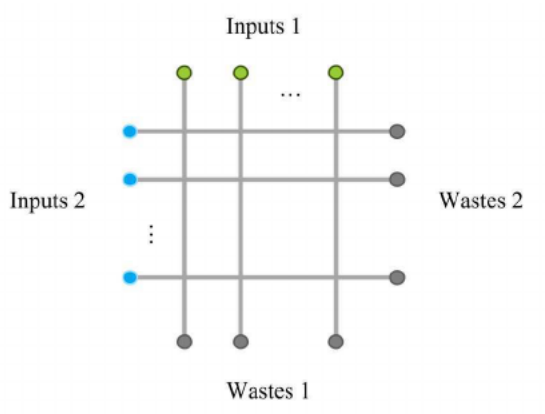

Fig. 1. Schematic of multiplexed microfluidic matrix for high-throughput screening.

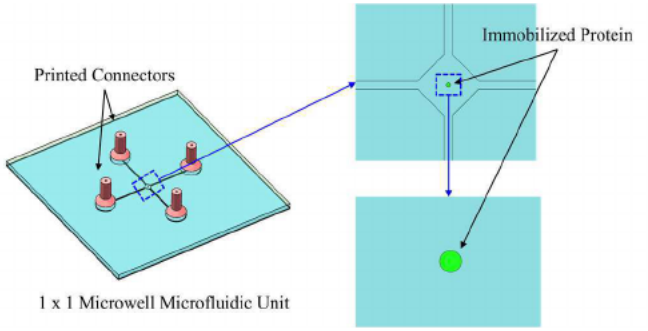

Fig. 2. Schematic of demonstrated 1 x 1 microwell immobilized protein assay with printed connectors in this study.

II. Materials & Methods

A. Materials

Photoresist (AZ4620, AZ Electronic Materials, Luxembourg) and developer (FHD-5, FUJIFILM Electronic Materials Co., Ltd, Japan) were used to fabricate the silicon mold. Trichloro (1H,1H,2H,2H-perfluorooctyl) silane 97% (Sigma-Aldrich, USA) was used to modify the silicon mold surface to make it hydrophobic. PDMS (SYLGARD 184) was purchased from Dow Corning Corporation, USA. For glass functionalization, (3-Aminopropyl)triethoxysilane (APTES) and tween-20 were purchased from Sigma-Aldrich, USA. 1-Ethyl-3-(3-dimethylaminopropyl)carbodiimide (EDC), N-Hydroxysuccinimide (NHS), mPEG-silane (MW = 1000), phosphate buffered saline (PBS), and 2-(N-morpholino)ethanesulfonic acid (MES) were purchased from Aladdin, China. The fluorescent-labeled protein, FITC-BSA, was purchased from Thermal Fisher Scientific, USA. The printing material, LOCTITE 3491, was purchased from Henkel AG & Company, Germany.

B. Preparation of PDMS Channels/Stamps

PDMS channels and stamps were prepared using a standard soft lithography process, which involved using patterned silicon molds to transfer desired layouts onto PDMS parts. Two types of Si molds were fabricated for this study: convex molds for microwell channels and concave molds for microcontact printing. Fig. 3 shows the process flow for fabricating Si molds and PDMS parts.

After sulfuric cleaning (10:1 H_2SO_4:H_2O_2), Si wafers were spin-coated with a positive photoresist (AZ 4620) at a speed of 4000 rpm for 30 seconds. A 6 µm thick PR layer was formed on the wafers after soft-baking at 90°C for 30 seconds. The PR-coated wafers then underwent photolithography and develop steps to create patterns for etching. Following deep reaction ion etching (DRIE), the wafers were deposited with trichloro (1H,1H,2H,2H-perfluorooctyl) silane by vacuum evaporation for 1 hour.

For PDMS casting, a PDMS mixture (10:1) was poured onto the Si molds and degassed in a vacuum chamber. After 2 hours of curing at 80°C, the PDMS parts were diced into pieces (20 x 20 mm^2). Fig. 4 shows the PDMS channel layout, where the channel width is 100 µm and the crossed microwell is a diamond shape with a width of 500 µm. The diameter of the inputs/wastes is 500 µm, and 2 mm half-circles are designed for aligning. Fig. 5 shows the stamp layout, involving a single circle with the diameter of 100 µm and 4 alignment marks.

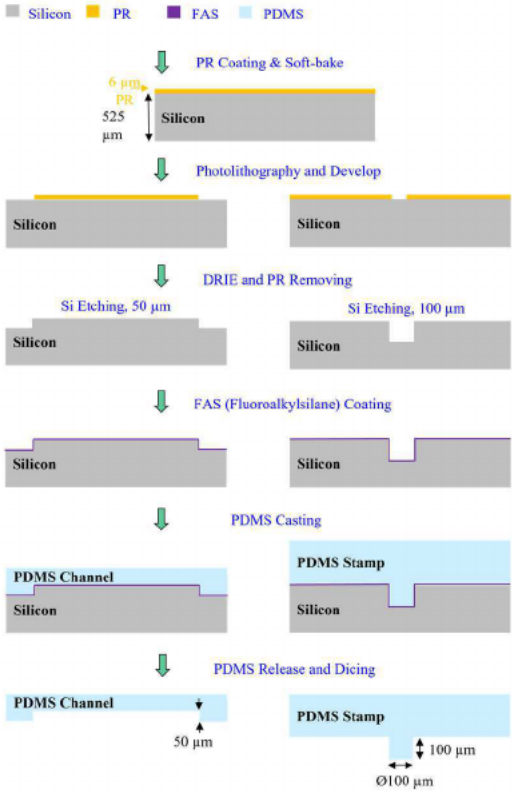

Fig. 3. Process flow for fabricating Si molds and PDMS parts.

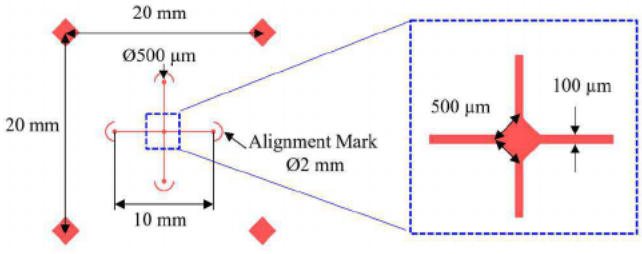

Fig. 4. Design layout of PDMS channels.

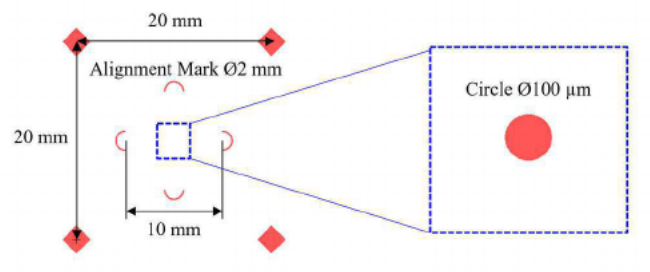

Fig. 5. Design layout of PDMS stamps.

C. Protein Immobilization on Glass

The procedure for protein immobilization on glass follows protocols described in published literature [16]. Glass substrates were cleaned with isopropanol (IPA) in an ultrasonic bath for 5 minutes, rinsed with deionized water (DI water), and then dried with N_2 gas. The glasses were then treated with O_2 plasma (100 W, 3 min) for surface hydroxylation.

Simultaneously, micropatterned stamps were inked with 20 µL of 2% APTES (dissolved in water) for 5 minutes. After drying with N_2 gas, the inked stamps were brought into contact with the plasma-treated glasses for 15 seconds. To minimize non-specific adsorption, the APTES-patterned glasses were subsequently treated with a 2% mPEG-silane solution (dissolved in water) for blocking.

Finally, the APTES-patterned glasses were incubated with an EDC/NHS activated protein solution for protein immobilization via covalent bonding for 30 minutes at room temperature (RT). For EDC/NHS activation, the protein solution was mixed with an EDC/NHS (1:1, 20 mg/mL) mixture for 30 minutes at RT. To demonstrate protein immobilization, we used a fluorescent-labeled protein, FITC-BSA (excitation/emission, 491/515 nm), at a concentration of 1 mg/mL in our experiments.

D. Assembly of Immobilized Protein Microfluidic Assay

The assembly process for immobilized protein assays is depicted in Fig. 6. Openings were drilled on the glass substrates for subsequent connector printing. A UV-assisted coaxial printing system was used for direct printing of microfluidic connectors. During printing, the coaxial nozzle deposited two types of materials, where the outer fluid was UV-curable adhesive, and the inner fluid was sacrificial water. The UV-curable adhesive was cured as a cylindrical hollow tube, while the water passed through the openings for drainage. Details of the printing process can be found in our previous papers [14].

After connector printing, APTES was patterned onto the other side of the glass substrates using the µCP method mentioned above. Then, after O_2 plasma treatment (100 W, 3 min), the APTES-patterned glass with printed connectors and the prepared PDMS channel substrates were bonded together to form a unit. Blocking was performed by flowing a mPEG-silane solution into the channel to block the un-patterned area for protein adsorption. Lastly, the protein solution was activated with an EDC/NHS mixture and flowed into the channel for protein immobilization.

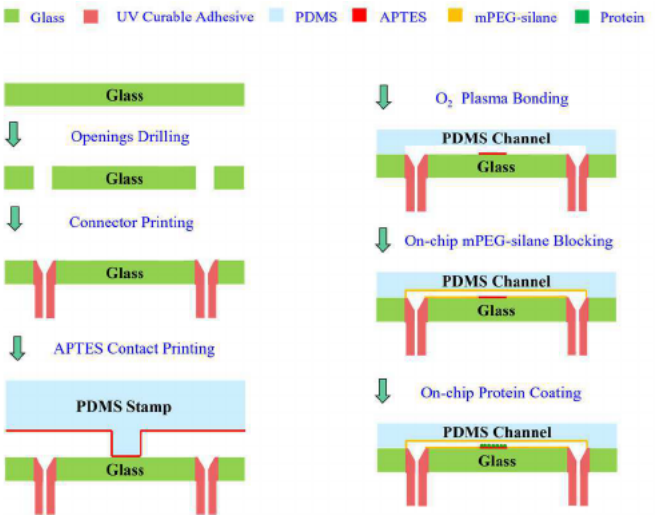

Fig. 6. Assembly process for 1 x 1 microwell immobilized protein assays with printed connectors.

III. Results & Discussions

To ensure the effectiveness of chemical grafting with relative treatments, we conducted water contact angle measurements and performed certain characterizations and experimental trials. As shown in Fig. 7, the water contact angle of untreated glasses was approximately 25°. We then treated the glasses with oxygen plasma for 3 minutes at 100 W, which decreased the water contact angle to approximately 9° due to the existence of hydroxyl groups on the surfaces. The plasma-treated glasses were subsequently soaked in a 2% APTES solution for 1 hour. The water contact angle increased to approximately 91°, representing the successful grafting of the APTES linker.

Then, we assembled the 1 x 1 microwell immobilized protein assays with 4 printed connectors, serving as interconnections at inputs or wastes. 1 x 1 microwell PDMS channels and single-circle PDMS stamps were prepared by soft lithography process described in Fig. 3. Glass substrates were drilled with 4 openings, and printed connectors were directly printed on the openings.

Four half-circle alignment marks were designed to fit the openings on glass. With their assistance, a single-circle APTES pattern was contact printed onto the microwell region of glass substrates with printed connectors. By O_2 plasma treatment, the patterned glass with printed connectors was bonded to the 1 x 1 microwell channel substrate to form a unit.

Subsequently, a 2% mPEG-solution and EDC/NHS activated FITC-BSA solution were flowed into the channel to finish blocking and protein immobilization. Fig. 8a shows an overview picture of the microfluidic unit filled with red ink, while Fig. 8b and 8c are the zoom-in views of a printed connector and the crossed microwell, respectively. The inner diameter of the connectors is approximately 240 µm, and the outer diameter is approximately 1 mm. Fig. 8d is the fluorescence image of the immobilized FITC-BSA circle (Ø100 µm) inside the microwell region (500 x 500 µm).

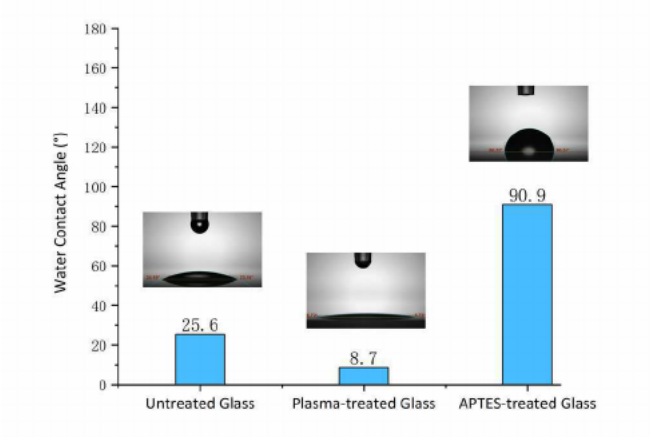

Fig. 7. Water contact angle measurements of glasses with relative treatments.

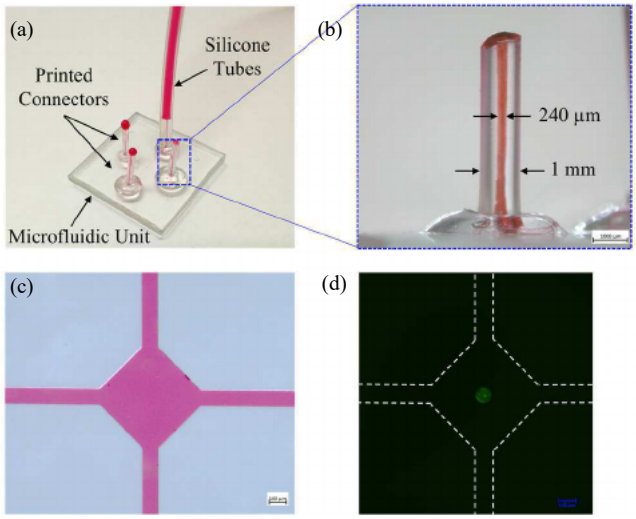

Fig. 8. (a) Overview picture of the 1 x 1 microwell immobilized protein assay; (b) zoom-in view of a printed connector; (c) zoom-in view of the crossed microwell; (d) the fluorescence image of the immobilized FITC-BSA circle (Ø100 µm) inside the microwell region (500 x 500 µm).

IV. Conclusions

The use of microfluidics for biological applications, particularly for high-throughput screening and multiplexing, has become increasingly popular. However, conventional interconnect techniques are limited in their ability to fabricate the hundreds or thousands of microfluidic interconnects needed for high-throughput microfluidics.

To address this challenge, coaxial printing as a rapid, customizable, and scalable technique was developed for microfluidic interconnects. The assembly process for immobilized protein microfluidic assays is detailed, including the use of printed connectors for interconnections at inputs or wastes, the protein immobilization methods via chemical grafting and the protein patterning with microcontact printing. The paper demonstrates the successful immobilization of protein into a 1 x 1 microwell microfluidic unit with printed connectors. For further studies, functional proteins such as antigens or antibodies can be immobilized into the device for detection. Additionally, future studies can extend the microfluidic unit to n x n microwells for high-throughput screening applications towards protein-to-protein and protein-to-cell interactions.

Overall, the paper provides valuable insights into the use of coaxial printing for microfluidic interconnects and the assembly process of them for immobilized protein microfluidic assays.

References

[1] S. T. Sanjay *et al.*, "Recent advances of controlled drug delivery using microfluidic platforms," *Adv. Drug Deliv. Rev.*, vol. 128, pp. 3–28, Mar. 2018, doi: 10.1016/j.addr.2017.09.013.

[2] S.-M. Yang, S. Lv, W. Zhang, and Y. Cui, "Microfluidic Point-of-Care (POC) Devices in Early Diagnosis: A Review of Opportunities and Challenges," *Sensors*, vol. 22, no. 4, pp. 1-33, Feb. 2022, doi: 10.3390/s22041620.

[3] S. Haeberle and R. Zengerle, "Microfluidic platforms for lab-on-a-chip applications," *Lab Chip*, vol. 7, no. 9, pp. 1094–1110, 2007, doi: 10.1039/b706364b.

[4] M. Yew, Y. Ren, K. S. Koh, C. Sun, and C. Snape, "A Review of State-of-the-Art Microfluidic Technologies for Environmental Applications: Detection and Remediation," *Glob. Challenges*, vol. 3, no. 1, pp. 1-13, Jan. 2019, doi: 10.1002/gch2.201800060.

[5] S. Halldorsson, E. Lucumi, R. Gómez-Sjöberg, and R. M. T. Fleming, "Advantages and challenges of microfluidic cell culture in polydimethylsiloxane devices," *Biosens. Bioelectron.*, vol. 63, pp. 218–231, Jan. 2015, doi: 10.1016/j.bios.2014.07.029.

[6] G. Du, Q. Fang, and J. M. J. den Toonder, "Microfluidics for cell-based high throughput screening platforms—A review," *Anal. Chim. Acta*, vol. 903, pp. 36–50, Jan. 2016, doi: 10.1016/j.aca.2015.11.023.

[7] A. Sontheimer-Phelps, B. A. Hassell, and D. E. Ingber, "Modelling cancer in microfluidic human organs-on-chips," *Nat. Rev. Cancer*, vol. 19, no. 2, pp. 65–81, Feb. 2019, doi: 10.1038/s41568-018-0104-6.

[8] A.-G. Niculescu, C. Chircov, A. C. Bîrcă, and A. M. Grumezescu, "Fabrication and Applications of Microfluidic Devices: A Review," *Int. J. Mol. Sci.*, vol. 22, no. 4, pp. 1–26, Feb. 2021, doi: 10.3390/ijms22042011.

[9] S. Alom Ruiz and C. S. Chen, "Microcontact printing: A tool to pattern," *Soft Matter*, vol. 3, no. 2, pp. 168–177, 2007, doi: 10.1039/B613349E.

[10] A. C. Glavan *et al.*, "Rapid fabrication of pressure-driven open-channel microfluidic devices in omniphobic RF paper," *Lab Chip*, vol. 13, no. 15, pp. 2922–2930, 2013, doi: 10.1039/c3lc50371b.

[11] Eden Tech, "Connector Kit." https://eden-microfluidics.com/eden-materials/luer-lock/.

[12] A. Chen and T. Pan, "Fit-to-Flow (F2F) interconnects: Universal reversible adhesive-free microfluidic adaptors for lab-on-a-chip systems," *Lab Chip*, vol. 11, no. 4, pp. 727–732, 2011, doi: 10.1039/c0lc00384k.

[13] Z. Yang and R. Maeda, "Socket with built-in valves for the interconnection of microfluidic chips to macro constituents," *J. Chromatogr. A*, vol. 1013, no. 1–2, pp. 29–33, 2003, doi: 10.1016/S0021-9673(03)01125-7.

[14] Q. Xu, J. C. C. Lo, and S. W. R. Lee, "Directly printed hollow connectors for microfluidic interconnection with UV-assisted coaxial 3D printing," *Appl. Sci.*, vol. 10, no. 10, pp. 1–13, 2020, doi: 10.3390/APP10103384.

[15] Q. Xu, J. C. C. Lo, and S. W. R. Lee, "Characterization and evaluation of 3D-printed connectors for microfluidics," *Micromachines*, vol. 12, no. 8, 2021, doi: 10.3390/mi12080874.

[16] H. Li *et al.*, "Aminosilane micropatterns on hydroxyl-terminated substrates: Fabrication and applications," *Langmuir*, vol. 26, no. 8, pp. 5603–5609, 2010, doi: 10.1021/la9039144